Palaeogeography, Palaeoclimatology, Palaeoecology 435 (2015) 167–176

Contents lists available at ScienceDirect

Palaeogeography, Palaeoclimatology, Palaeoecology

journal homepage: www.elsevier.com/locate/palaeo

Reconstruction of a paleotemperature record from 0.3–3.7 ka for subtropical South China using lacustrine branched GDGTs from Huguangyan Maar

Jianfang Hu [a,b,*], Haoda Zhou [a], Ping'an Peng [a], Xiaoqiang Yang [c], Baruch Spiro [d], Guodong Jia [b], Gangjian Wei [b], Tingping Ouyang [b]

[a] State Key Laboratory of Organic Geochemistry, Guangzhou Institute of Geochemistry, Chinese Academy of Sciences, Guangzhou 510640, PR China
[b] CAS Key Laboratory of Marginal Sea Geology, Guangzhou Institute of Geochemistry, Chinese Academy of Sciences, Guangzhou 510640, PR China
[c] Department of Earth Sciences, Sun Yat-Sen University, Guangzhou 510275, PR China
[d] Department of Mineralogy, The Natural History Museum, Cromwell Road, London SW7 5BD, UK

ARTICLE INFO

Article history:
Received 27 October 2014
Received in revised form 29 April 2015
Accepted 9 June 2015
Available online 17 June 2015

Keywords:
GDGTs
China
Paleoclimate
Maar lake
MBT
CBT

ABSTRACT

The concentrations of glycerol dialkyl glycerol tetraethers (GDGTs) in catchment soils, suspended particulate matter (SPM), lake bottom sediments, and sediment cores from Huguangyan Maar, subtropical South China, were investigated. The distribution of isoprenoid GDGTs has GDGT-0/crenachaol > 2 and therefore the widely used TEX_{86} is precluded from being used for the calculation of lake water temperature in this lake. The total concentration of branched GDGTs (br-GDGTs) in the soils, SPM, and lake bottom sediments ranged from 91.3–223.7 ng/g, 17.8–41.4 ng/L, and 864.2–2008.6 ng/g, respectively. The molecular composition of br-GDGTs, MBT values (methylation of br-GDGTs), and CBT values (the cyclization ratio of br-GDGTs) in the catchment soils differ from those in lake materials. This difference indicates that br-GDGTs in the lake are largely produced *in situ*. Based on the global lake-specific MBT/CBT–MAT (mean air temperature) calibration, the air temperature was reconstructed for lacustrine material in Huguangyan Maar. The estimates fall in the range 23.2–23.8 °C, similar to the average value of local MAT for the preceding 45 years. The paleotemperature history of Huguangyan Maar was reconstructed using br-GDGTs extracted from a sediment core spanning the period 0.3–3.7 ka, and ranged from 24.6 to 26.3 °C. The temperature pattern of Huguangyan Maar based on the global lake-specific MBT/CBT–MAT resembles those recorded in East China using numerous indicators. The pattern consists of five cool and four warm periods, including two distinct phases within the Medieval Warm Period (900–1300 AD), the coldest temperature in the Little Ice Age (1550–1850 AD) and reveals even finer temperature variations than other indicators. This new method based on br-GDGTs, produced *in situ* in the subtropical lacustrine environment, provides a new sensitive and precise paleotemperature proxy for lacustrine sediments for which other GDGT-based proxies are not applicable.

1. Introduction

Glycerol dialkyl glycerol tetraethers (GDGTs) are membrane lipids produced by archaea and bacteria (Sinninghe Damsté et al., 2000; Weijers et al., 2006a; Schouten et al., 2013) and exist in two major forms: isoprenoid and branched (Appendix). Isoprenoid GDGTs are produced by various archaea and occur mostly in the form of acyclic or ring-containing biphytanyl chains (De Rosa and Gambacorta, 1988; Koga and Morii, 2006). Branched GDGTs are generally attributed to soil bacteria (Weijers et al., 2006b) and possibly to Acidobacteria (Sinninghe Damsté et al., 2011).

The distribution patterns of GDGTs in lacustrine sediments have been used as indicators for lake water temperature and/or mean annual air temperature (MAT) as the compositions of both isoprenoid and branched GDGTs have been found to be temperature dependent (Schouten et al., 2002; Weijers et al., 2007a). One such indicator, TEX_{86} (TetraEther indeX of tetraethers consisting of 86 carbon atoms; Schouten et al., 2002), has been used successfully in the reconstruction of long, high-resolution temperature records from tropical African lake sediments (Powers et al., 2005; Tierney et al., 2008). However, it has been found that TEX_{86} only works in large lakes having high proportions of isoprenoid to branched GDGTs (Blaga et al., 2009; Powers et al., 2010).

* Corresponding author at: Guangzhou Institute of Geochemistry, Chinese Academy of Sciences, Guangzhou, GD 510640, PR China. Tel.: +86 20 85290163; fax: +86 20 85290117.
E-mail address: hujf@gig.ac.cn (J. Hu).

http://dx.doi.org/10.1016/j.palaeo.2015.06.014
0031-0182/

Another proxy used for the estimation of past MAT is primarily based on branched GDGTs in soils (Weijers et al., 2007b). This proxy quantifies the extent of methylation of branched tetraethers (MBT) and the cyclization ratio of branched tetraethers (CBT). It was found that CBT is primarily related to the pH of the soil, and that MBT is positively correlated with MAT and, to a lesser extent, negatively correlated with the pH of the soil (Weijers et al., 2007b). When both parameters are combined, it appears that the variation in the MBT is largely explained by both MAT and pH (Weijers et al., 2007b). Recent studies have shown that values of MBT/CBT are significantly correlated with those of MAT in lakes, as for example in East Africa (Tierney et al., 2010) and New Zealand (Zink et al., 2010). These correlations highlight the potential for branched GDGTs to be used as temperature proxy indicators in various lacustrine settings. However, its application in lakes seems to be complicated by *in situ* production of branched GDGTs in the water column and /or the bottom sediments (Tierney and Russell, 2009; Tierney et al., 2010; Loomis et al., 2011; Sun et al., 2011). Furthermore, it has been noted that local or regional calibrations may be necessary for reconstructing absolute MAT histories (Schouten et al., 2013). Therefore, several lake-specific calibrations have been developed which incorporate the potential aquatic input of branched GDGTs and thus enable the reconstruction of paleotemperatures based on branched GDGTs in lake sediments (Tierney et al., 2010; Sun et al., 2011; Loomis et al., 2012). Another GDGT proxy, the BIT (branched/isoprenoid) index, has been proposed and applied to the determination of the relative inputs of soil organic matter to aquatic environments (Hopmans et al., 2004; Weijers et al., 2007a; Walsh et al., 2008).

Despite the fact that *in-situ* production of branched GDGTs likely occurs in variable abundances in different lakes, several lacustrine studies suggest that it is still possible to reconstruct MAT histories using the MBT/CBT proxies (e.g. Zink et al., 2010; Fawcett et al., 2011). Many uncertainties currently exist regarding sources of branched GDGTs found in lakes and thus in the use of MBT/CBT as a paleothermometer of lakes. In order to improve the reliability of GDGT-based proxies in lakes, it is necessary to better understand the sources of the GDGTs in lacustrine systems. Although several temperature reconstructions by different indicators have been published for the east and north of China (Chu, 1973; Zhang, 1996; Zhang et al., 2000; Wang et al., 2001; Yang et al., 2002; Ge et al., 2003), so far none has been published for South China. Therefore, this study aims to: 1) investigate the distribution and concentrations of GDGTs in the sedimentary archive of Huguangyan Maar (a small-medium size lake) in subtropical South China, 2) identify their sources and determine their respective pathways, and 3) carry out appropriate calibrations for estimating the local air temperature over the past ~3700 years. This study should improve the basis for the application of these methods and the interpretation of the analytical results in terms of paleotemperature as recorded by GDGTs in lacustrine sediments.

2. Site location and modern climate

2.1. Site location

The freshwater meromictic Huguangyan Maar (21°9′N, 110°17′E) is located approximately 15 km southwest of Zhanjiang on the Leizhou Peninsula, Guangdong Province in the subtropical region of South China (Fig. 1). The lake has a surface area of 2.3 km^2 and a maximum depth of 20 m. The catchment area (3.5 km^2) comprises only the inner slopes of the crater rim. The lake has no defined surface inflow or outflow (Chu et al., 2002), and its thermocline remains between 6 and 13 m depth. The lake is a closed maar lake, with a crater basin that was created by basaltic phreatomagmatic eruptions 140 ka ago (Liu, 1999). The tephra ring of pyroclastic sediments is 10–58 m above the lake surface (Chu et al., 2002).

2.2. Modern climate

The Huguangyan Maar setting has a subtropical climate regime of the East Asian monsoon, which is characterized by northern cold fronts originating from the Siberian anti-cyclone during the winter, and the Asian Southwest and Southeast summer monsoon from the Pacific Ocean. The climate in this area is strongly seasonal, with 90% of the total mean annual precipitation of ca. 1570 mm falling between April and October (Chu et al., 2002) and a dry season from November to March. The air temperature is also seasonal, with the highest temperature occurring between July and August and the lowest temperature occurring in January. Abnormally high temperatures could reach 38.8 °C and abnormally low temperatures can reach as low as −1.4 °C (Wang et al., 2000). For the last 45 years, the MAT for Zhanjiang (15 km from Huguangyan) has been 23.1 °C (Mingram et al., 2004). In biogeographical terms, the lake now belongs to a zone of subtropical grassland, and the natural vegetation is that of a tropical semi-evergreen seasonal rain forest (Zheng and Lei, 1999).

3. Material and methods

3.1. Sample collection

Sediment cores, HGY-2 (1.67 m in length), HGY-6 (3.68 m in length), and HGY-7 (3.68 m in length) (21°08.588′N, 110°16.651′E) were collected from Huguangyan Maar at ~10 m water depth (Fig. 1) using a modified Livingstone piston corer in November 2009. These cores were taken within an area of ~20 m^2. The top ~19.5 cm of sediment in cores HGY-2 and HGY-6 was lost because of high water content. To avoid this problem, Core HGY-7 was taken starting at ~1.5 m below the sediment surface. Core HGY-2 was selected for the present study. The cores were split and one half was sampled at ~1 cm intervals, about 160 samples were produced and immediately stored at −20 °C prior to their analysis.

In order to help identify the source of GDGTs (autochthonous and allochthonous) in Huguangyan, six surface sediments, three samples of suspended particulate matter (SPM) and four soil samples from around the lake were collected for study and comparison of GDGTs. Samples of top soils (0–10 cm) were collected at four locations close to the lake in March 2010. At each one of the four locations (Fig. 1), several subsamples were collected and then pooled to yield a representative sample. All of the soil samples were collected using a clean stainless steel shovel, and all collected samples were wrapped in solvent-cleaned aluminum foil and stored at −20 °C until analysis. Lake bottom sediments (0–3 cm) were collected with a grab sampler. Sampling of SPM was performed along a vertical profile in the center of the lake on March 13, 2010. Water samples (20–30 L) collected with 8 L Niskin bottles were taken at 0.5 m, 6 m, and 18 m water depth at one location. Within 8 h, the water samples (25 L each) were filtered through Glass Fiber Filters (GFF) (0.7 μm, Whatman) and the filtrates were stored frozen, until processing.

3.2. GDGT analysis

Soils and sediments were freeze-dried and ground into fine powder, spiked with an appropriate amount of C_{46}-GDGT (standard compound) and extracted with an azeotropic mixture of dichloromethane/methanol (2/1, v/v) in a Soxhlet apparatus for 72 h. The GFF filters containing SPM were extracted in an ultrasonic bath using a stepwise extraction procedure with 9 steps covering a range from 100% methanol to 100% DCM. All extracts were rotary evaporated to dryness and then redissolved in a small amount of hexane/DCM mixture (9:1, v/v). The extracts were fractionated by column chromatography on neutral alumina. The apolar fraction and polar fraction were eluted using hexane/DCM (9:1, 60 mL) and DCM/methanol (1:1, 70 mL), respectively. The polar fraction was recovered by rotary evaporation, dissolved in

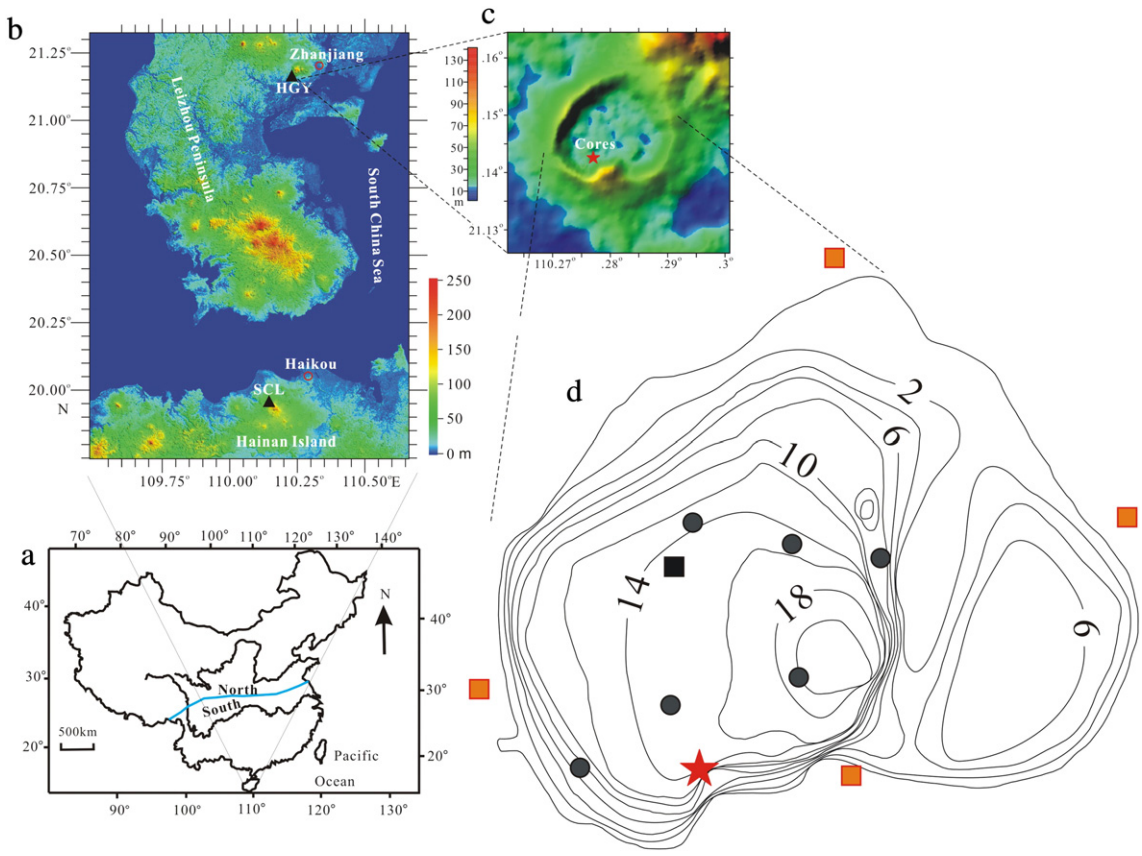

Fig. 1. (a) Map of the study area in South China; (b) location of Huguangyan and Shuangchiling (SCL) maar lakes (color indicates elevation); (c) the site of cores in Huguangyan Maar (color indicates elevation, Yang et al., 2012); and (d) locations of samples: ★ site of the cores, ■ sampling sites of soil, ■ sampling site of suspended particulate matter (SPM), ● sampling sites of bottom surficial sediments, the contours indicate water depth (m).

hexane/isopropanol (99:1, v/v), and filtered through a 0.45-μm polytetrafluoroethene (PTFE) filter prior to analysis by high-performance liquid chromatography/atmospheric pressure chemical ionization mass spectrometry (HPLC/APCI-MS, Zhou et al., 2014).

Analyses were performed using an Agilent 1200 series liquid chromatography equipped with an auto-injector and ChemStation chromatography management software. Separation was carried out with a Prevail Cyano column (2.1 mm × 150 mm, 3 μm; Alltech, Deerfield, USA) kept at 30 °C. GDGTs were eluted isocratically with 99% hexane and 1% propanol for 5 min, followed by a linear gradient to 2% propanol over 40 min. The flow rate was 0.2 mL/min. Identification was performed using a positive ion chemical ionization-Agilent 6410 triple quad mass spectrometer (APCI-MS) under atmospheric pressure. The conditions were: nebulizer pressure 60 psi; vaporizer temperature 300 °C; drying gas (N_2), flow rate 5 L/min, temperature 200 °C; capillary voltage 2500 V; and corona 5 μA. GDGTs were detected *via* single-ion monitoring (SIM) of their $[M + H]^+$ and $[M + H]^+ + 1$ and quantification was achieved by integration of the peak areas (Schouten et al., 2007). Absolute concentrations were calculated using the internal standard material (C_{46}-GDGT), following Huguet et al. (2006). The relative response factors (RRF) of each GDGT and the internal standard material were not measured, so only semi-quantitative results were achieved. However, as CBT/MBT values, which are the ratios of similar compounds, should not be affected. Each sample was analyzed in duplicate, and the data presented are averages of the duplicates. The precisions of CBT and MBT computation are 0.014 and 0.008, respectively, and that of the MAT values obtained by conversion is ±0.4 °C for both. Replicate analysis of samples shows that the reproducibility of BIT index measurements is ±0.03.

4. Results and discussion

4.1. Core chronology

The chronology of composite profiles HGY-2 & HGY-7, and HGY-6 & HGY-7 was presented by Yang et al (2012). Radiocarbon (AMS ^{14}C) ages and volume magnetic susceptibility correlation between HGY-2 and HGY-7 cores show some overlap (Fig. 2). When analyzing the pattern of magnetic susceptibility curves and cycling variations, we identified several notable high and low values of the HGY-2 profile with letters A ~ G, and then the tie points D ~ G on the HGY-7 profile can easily be recognized (Fig. 2). Consequently, two radiocarbon ages 2.04 cal kyr and 2.79 cal kyr of core HGY-7 can be integrated into the profile of HGY-2 at 135 cm and 162 cm, respectively. However, four radiocarbon ages are insufficient to construct a high-resolution chronology. The top sediments were absent, and therefore the radiocarbon ages could not be constrained. We compared the paleosecular variations of HGY-2 with the records of Shuangchiling lake sediments and Chinese paleomagnetic materials, as well as CALS7K.2 model curves (Lund et al., 2006; Yang et al., 2009). The top sediments of HGY-2 could then be constrained to about 0.2–0.4 cal kyr (Yang et al., 2012). The mean value ~0.3 cal kyr can serve as an estimated age of the top sediments.

On the basis of the radiocarbon ages and volume magnetic susceptibility correlation between cores HGY-2 and HGY-7, four ages and the estimated age (0.3 kyr) of the top of HGY-2 could be used to construct the chronology of the core HGY-2 by linear interpolation (Table 1). The results indicate that sediments of the HGY-2 core have been accumulating since ~3.7 ± 0.1 cal kyr. We further correlated the magnetic susceptibility curves of HGY cores to previously published results (Yancheva et al,

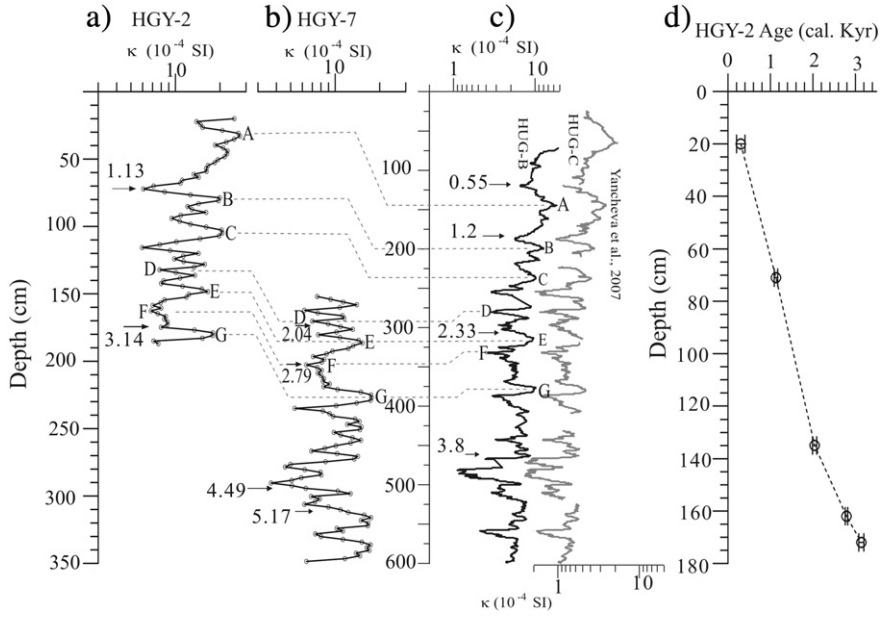

Fig. 2. Depth profile of magnetic susceptibility for cores HGY-2 (a), HGY-7 (b), HUG-B and HUG-C (c) (Yancheva et al., 2007). The capital letters indicate the tied layers. Short arrows in (a), (b) and (c) indicate the radiocarbon dating points; (d) shows the age–depth model of the composite profile, and short vertical double lines besides the data symbols show age errors.

2007). As shown in Fig. 2, the tie points A–G in the HGY-2 core can also be identified in their counterparts in HUG-B and HUG-C cores (Yancheva et al., 2007). Overall, the agreement of ages between the different profiles corroborates the reliability of the chronology of HGY-2 profile.

4.2. GDGT distribution in and around the Huguangyan Maar

Although branched GDGTs have attracted attention as a potential new proxy for paleotemperature for continental climate reconstruction (Blaga et al., 2010), the sources of branched GDGTs in lake sediment remain unclear, although both allochthonous inputs (delivered *via* soil runoff) and autochthonous inputs (produced within the water column and/or the lake sediment itself) are possible sources. In order to identify the sources of branched GDGTs in Huguangyan sediments, we compared the GDGT compositions and variability in soils around the lake, and the lake materials (SPM and lake bottom sediments).

4.2.1. GDGTs in soils

Four soil samples collected from sites around the lake (Fig. 1) were analyzed to investigate the GDGT distribution in soils within the lake catchment and to determine the terrestrial GDGT end member. The concentrations of isoprenoid GDGTs in soils range between 1.8 and 8.5 ng/g dry weight (dw), and that of branched GDGTs are between 91.3 and 223.7 ng/g. The GDGT compositions are dominated by branched GDGTs (up to 99.2% of total GDGTs) (Table 2; Fig. 3a). For the branched GDGTs in soil, the average proportions of GDGTs-I, II, and III are 83.3, 5.7, and 0.4%, respectively (Fig. 3c), which are similar to the values reported previously from soil samples collected globally (Weijers et al., 2007b).

The isoprenoid GDGTs are dominated by crenarchaeol and the TEX_{86} values are 0.64–0.89, suggesting that Thaumarchaeota are the dominant archaea in the soil surrounding the lake, where they play an important role in the N cycle (e.g. Ochsenreiter et al., 2003). The proportion of the crenarchaeol isomer (relative to crenarchaeol) is around 10% for the soils, indicating that group 1.1b Thaumarchaeota that produce more crenarchaeol isomer (Sinninghe Damsté et al., 2012) are predominant in the soils surrounding Huguanyan Maar. The BIT values range from 0.94 to 1.00. The reconstructed pH values are from 5.9 to 6.3 (Table 2), which are in the range of values of soil pH in the Zhanjiang area (Guo et al., 2011). The MAT calculated using the soil-based MBT/CBT calibration (Weijers et al., 2007b) ranges from 29.3–31.3 °C, which is higher than the local MAT (23.1 °C). It seems, therefore that there are additional environmental factors other than temperature and pH that influence the distribution of branched GDGTs; possibly soil moisture, nutrient conditions, or soil type. An alternative explanation might be that in this case, the composition of branched GDGTs is determined by the composition of the microbial community rather than by membrane adjustment to changing environmental conditions; not all strains of branched GDGT-producing bacteria may generate the same branched GDGT pattern at the same temperature (Naeher et al., 2014).

4.2.2. GDGTs in suspended particulate matter (SPM) and lake sediment

The concentrations of isoprenoid GDGTs in SPM samples (collected at the surface — 0.5 m, middle — 6 m depth and the bottom — 18 m depth) vary between 65.8 and 140.6 ng/L, accounting for 72.5–84.5% of the total GDGTs. The total branched GDGT concentrations vary between 17.8 and 41.4 ng/L. The relative abundances of isoprenoid and branched GDGTs at the three different depths in the water column are similar (Fig. 3a), and GDGT-0 dominates at all depths (Fig. 3b). In the SPM collected at 18 m, GDGT-0 was more abundant than at the other two depths (weighted average 69.6% of total GDGTs at 18 m compared to 59.2% at 6 m and 58.6% at 0.5 m). The percentages of GDGTs-I, II, and III in SPM are between 39.2% and 43.1%, between 25.4% and 27.7%, and between 5.9% and 7.8% for the three depths, respectively. The absolute

Table 1
Radiocarbon ages. All carbon ages were calibrated using the program CalPal with calibration curve INTCAL98 (www.calpal.de).

Depth (cm)	Materials	Cal ^{14}C Age (kyr)	Cal ^{14}C Error (kyr)	Correlation Error (kyr)	Method
20		0.3		0.1	Correlation
71	Plant debris	1.13	0.04		AMS^{14}C
135	Leaf	2.04	0.05	0.1	AMS^{14}C, correlation
162	Plant debris	2.79	0.03	0.05	AMS^{14}C, correlation
172	Plant debris	3.14	0.06		AMS^{14}C

Table 2
Absolute concentrations of individual branched GDGTs, total branched GDGTs and total isoprenoid GDGTs, BIT, TEX_{86}, CBT and MBT, and MBT/CBT-reconstructed mean air temperature (MAT) for the modern samples presented.

Sample set	Sample no.	Individual branched GDGT concentration (ng/g)									Branched GDGTs concentration (ng/g)	Isoprenoid GDGTs concentration (ng/g)	BIT	TEX_{86}	CBT	MBT	pH	MBT/CBT–MAT (°C)
		III	IIIb	IIIc	II	IIb	IIc	I	Ib	Ic								
Soils	S1	1.4	0.1	0.0	12.7	2.4	0.7	113.8	12.3	3.4	146.8	6.7	0.99	0.67	0.94	0.88	6.3	29.3[a]
	S2	0.2	0.0	0.0	4.8	0.7	0.08	81.9	8.0	1.8	97.5	4.8	0.97	0.78	1.00	0.94	6.1	31.3[a]
	S3	0.4	0.04	0.0	8.3	1.4	0.2	196.6	13.4	3.4	223.7	1.8	1.00	0.64	1.14	0.95	5.9	30.9[a]
	S4	0.3	0.0	0.0	5.0	0.5	0.03	76.7	6.9	1.9	91.3	8.5	0.94	0.89	1.05	0.94	6.0	31.0[a]
Surface sediments	D1	35.2	6.9	1.1	230.1	95.3	14.3	302.1	155.9	44.8	885.7	66.3	0.98	0.48	0.33	0.57	7.9	23.8[b]
	D2	62.7	10.7	1.3	353.0	147.8	19.9	454.8	228.3	58.8	1337.3	94.3	0.98	0.40	0.33	0.55	7.9	23.3[b]
	D3	55.7	10.0	1.4	302.1	127.4	16.8	392.1	193.0	47.0	1145.5	93.9	0.98	0.38	0.34	0.55	7.9	23.2[b]
	D4	39.1	7.0	1.0	225.1	94.2	13.5	300.2	145.0	39.1	864.2	72.9	0.98	0.44	0.34	0.56	7.9	23.5[b]
	D5	76.2	12.4	2.4	435.6	186.4	25.9	550.6	285.2	75.7	1650.4	123.2	0.98	0.44	0.32	0.55	7.9	23.3[b]
	D6	103.3	13.1	1.5	529.7	216.9	26.5	716.7	335.8	65.0	2008.5	165.2	0.99	0.36	0.35	0.56	7.8	23.2[b]
SPM	0.5 m	2.7	0.0	0.0	11.6	4.0	0.6	19.6	5.9	1.0	45.4	119.5	0.84	0.40	0.49	0.59	7.5	23.6[b]
	6 m	1.9	0.0	0.0	7.8	2.6	0.3	12.3	3.7	0.9	29.5	109.2	0.84	0.60	0.50	0.58	7.4	23.2[b]
	18 m	2.7	0.0	0.0	9.4	3.1	0.3	13.4	4.5	0.7	34.1	185.5	0.82	0.44	0.48	0.55	7.5	22.1[b]

[a] MAT calculated according to Weijers et al.(2007b).
[b] MAT calculated according to Sun et al. (2011).

concentrations of branched GDGTs in the water column exhibit the pattern with surface > bottom > middle, but the isoprenoid GDGTs show the pattern with bottom > surface > middle (Table 2). Branched GDGTs containing one or two cyclopentyl moieties are less abundant in SPM than those without cyclopentyl moieties (Fig. 3c).

The BIT index values are 0.84, 0.84, and 0.82 at 0.5 m, 6 m, and 18 m water depth, respectively. These values are higher than those in coastal environments and some lakes (Powers et al., 2004; Blaga et al., 2009).

The TEX_{86} values for the SPM material sampled in March 2010 are 0.40, 0.60, and 0.44, and the TEX_{86}-derived (Castañeda and Schouten, 2011) lake water temperatures are 8.8 °C, 20.8 °C, and 10.8 °C for the three depths, respectively. However, the water temperatures measured during sampling were 18.5 °C, 18.3 °C, and 15.5 °C for the respective water depths during the SPM sampling in March 2010. Also, the average water temperatures during November 2008–May 2009 were 25.0 °C, 24.4 °C, and 20.6 °C for the surface, middle and bottom water depths, respectively (Wang et al., 2012). These data indicate that the TEX_{86} values cannot be used for the reconstruction of the lake water temperature in Huguangyan Maar (see Discussion in Section 4.4 below).

For the lake bottom sediments, the concentration of isoprenoid and branched GDGTs ranges from 66.3 to 165.2 ng/g and from 864.2 to 2008.6 ng/g dry weight (dw) respectively (Table 2). The GDGT distributions are dominated by branched GDGTs (92.2–93.4%, mean 92.8%). For branched GDGTs, the lake bottom sediments contain a high proportion of GDGT-I, followed by GDGT-II (Fig. 3c), which is similar to the distribution of branched GDGTs in surface sediments in low elevation lakes in western Uganda (Loomis et al., 2011). Branched GDGTs containing one or two cyclopentyl moieties are less abundant in surface sediments than those without cyclopentyl moieties (Table 2; Fig. 3c). The reconstructed pH values are 7.8–7.9, which are close to the measured water pH (7.7). The BIT values are high, varying from 0.98 to 0.99. The TEX_{86} values are 0.42 on average, and the temperatures derived from TEX_{86} (Castañeda and Schouten, 2011) are between 6.2–12.9 °C with an average of 9.5 °C.

The distributions of GDGTs in the sediment cores taken in the lake are similar to those of the samples of surficial lake bottom sediments. The concentrations of total branched GDGTs vary between 115.2 and 3061.6 ng/g, accounting for up to 93.9% of total GDGTs. The BIT values in the core sediments range from 0.96 to 1.00, and the CBT and MBT values are 0.29–0.45 and 0.59–0.65, respectively (Fig. 5a, b and c).

4.3. Sources of GDGTs in Huguangyan Maar

The distributions of isoprenoid GDGTs in SPM at the different water depths are almost identical (Fig. 3b), indicating a single type of source(s) for these components. This distribution, dominated by GDGT-0 and extremely low crenarchaeol, strongly suggests that isoprenoid GDGTs were derived mainly from methanogens (producing predominantly GDGT-0, Blaga et al., 2009) and were not from Thaumarchaeota in Huguangyan Maar. Thaumarchaeota are the only archaea identified as producers of crenarchaeol (Sinninghe Damsté et al., 2002; Schouten et al., 2008; Pitcher et al., 2010, 2011). Moreover, the amount of crenarchaeol isomer, which is very low for lake material (0–3.5%, relative to crenarchaeol), differs from that in surrounding soils, supporting the suggestion that some isoprenoid GDGTs are produced *in situ* in the lake. The average GDGT-0/crenarchaeol ratio of the SPM (23.7) is substantially higher than that of the average value for the lake bottom sediment (3.5), indicating that GDGT-0 was produced by methanogenic archaea in the water column. Blaga et al (2009) suggested that, if the GDGT-0/crenarchaeol ratio is >2, a non-Group I crenarchaeotal origin is evident for GDGT-0, and in such a case, it is not appropriate to calculate TEX_{86} values and infer past lake water temperatures. It is therefore concluded that TEX_{86} values cannot be used in the reconstruction of past water temperature in Huguangyan Maar.

Significant differences were recorded in both the concentrations and compositions of branched GDGTs between soils and lake materials (Fig. 3 and Table 2). Firstly, the concentrations of branched GDGT are significantly higher in the lake sediments than in soils (Table 2), which suggest that in addition to the soil, another source of branched GDGTs exists for lake sediment. Secondly, the mean values of the relative abundances of nine branched GDGTs in the soils are quite different from those of the lake bottom sediments (Fig. 3c). In Huguangyan Maar, the relative abundance of GDGTII and IIb is much higher in the sediments than in surrounding soil (Fig. 3c), supporting the suggestion that some branched GDGTs are produced *in situ* in lakes. Also Tierney et al. (2010) and Sun et al. (2011) found enhanced production of GDGTII and GDGTIII in sediments from certain lakes in tropical Africa and China, respectively, while Loomis et al. (2011) observed enhanced production of GDGTIII in high elevation lakes, in contrast to GDGTIand GDGTII in low elevation lakes from western Uganda. Therefore, we suggest that a variety of branched GDGTs can be produced *in situ* in the lacustrine environment *vs.* the surrounding soils.

Similar MBT and CBT values are observed in SPM and lake bottom sediments, and they are lower than those of the soil samples (Table 2). Moreover, the narrow range of the calculated pH values of 7.8–7.9 for the lake bottom sediments are similar to those calculated for the lake water (7.7), but are higher than the pH values of 5.9–6.3 for the soils (Table 2). This difference further suggests a substantial contribution of branched GDGTs originating from *in situ* production in the lake water column and/or in its bottom sediments. However, the exact

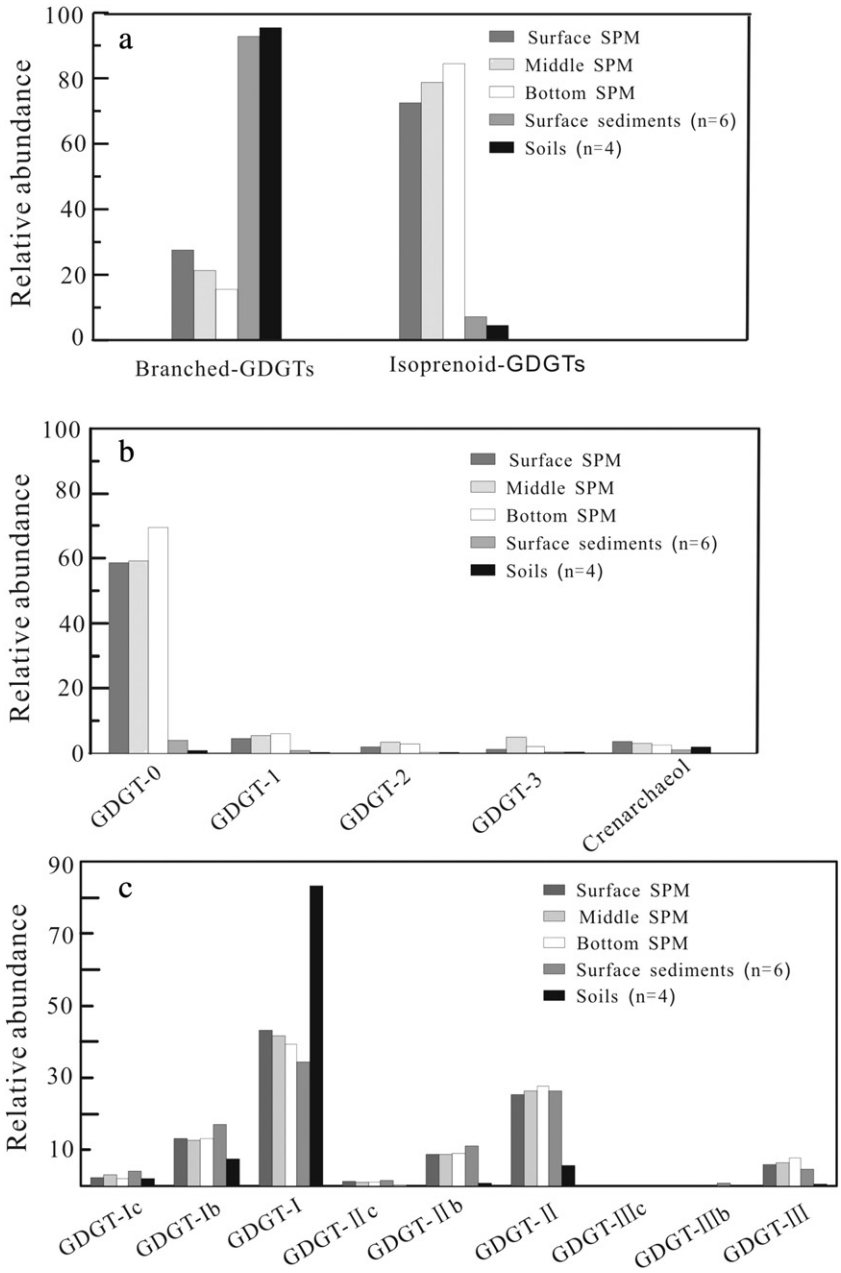

Fig. 3. Bar plots showing the average distribution for GDGTs for (a) branched and isoprenoid GDGTs in suspended particulate matter (SPM), surface sediments, and soils, (b) relative abundance of isoprenoid GDGTs; (c) relative abundance of nine branched GDGTs.

biological origin of the branched GDGTs is not been determined so far (e.g. Blaga et al., 2010).

These three lines of evidence indicate that the application of the MBT/CBT ratio as proxy for paleotemperature in the Huguangyan Maar requires an alternative calibration based on the distribution of branched GDGTs in the lake bottom sediments rather than in soils.

4.4. Paleotemperature reconstruction of Huguangyan Maar

4.4.1. Temperature calibration of suspended particulate matter and lake bottom sediments

In order to carry out an appropriate calibration for reconstructing past continental temperatures, we reconstructed the MAT and pH using the soil-based MBT/CBT calibration set of Weijers et al. (2007b). The soil-based MBT/CBT calibration is based on the current knowledge that the distribution of soil-derived GDGT membrane lipids can be used in paleoenvironmental studies to estimate past MAT and soil pH. The reconstructed SPM temperatures are 18.6 °C, 18.0 °C, and 16.7 °C (Fig. 4) and the pH values are 7.5, 7.4 and 7.5 at 0.5 m, 6 m, and 18 m water depth, respectively. The estimated temperatures from lake bottom sediments range from 18.4–19.2 °C (Fig. 4). The reconstructed temperatures differ from the mean annual air temperature (23.1 °C) for the past 45 years (Fig. 4) in Zhanjiang, 15 km away (Mingram et al., 2004).

Therefore, we applied lake calibrations that were tested for global use (*i.e.* Pearson et al., 2011; Sun et al., 2011) for the temperature reconstruction. Using the sediment-based MBT/CBT calibration model of Sun et al. (2011, where $T = 3.949 - 5.593 \times CBT + 38.213 \times MBT$), based on lakes from China and Nepal, the reconstructed temperatures were 23.6 °C, 23.2 °C, and 22.1 °C for SPM collected at 0.5 m, 6 m, and 18 m water depth, respectively (Table 2, Fig. 4). The reconstructed

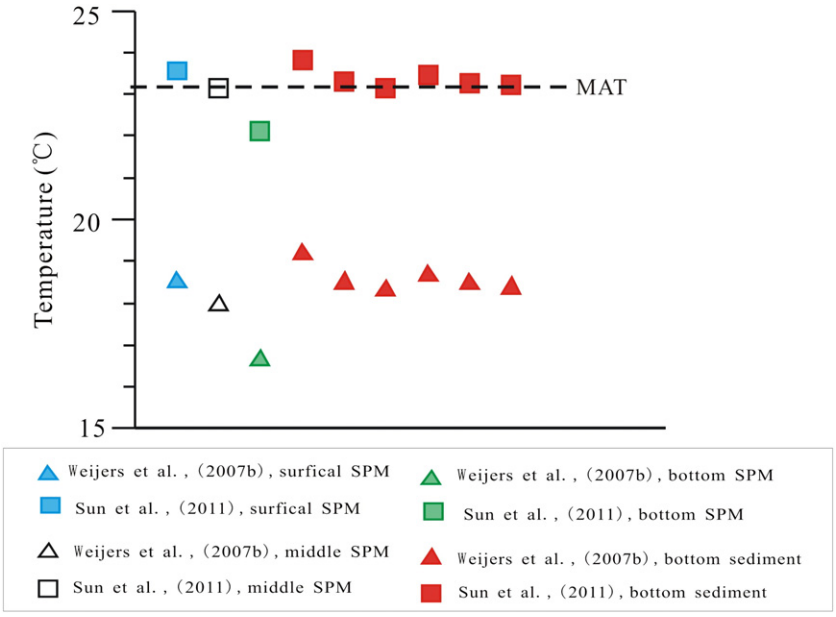

Fig. 4. Temperature estimates of SPM and bottom surficial sediments according to Weijers et al. (2007b) and Sun et al. (2011). For comparison with the derived temperature values, mean annual air temperature from Zhanjiang City was shown by – –.– –. Temperatures were calculated as: MBT = 0.122 + 0.187 × CBT +0.020 × T (Weijers et al., 2007b), and T = 3.949 − 5.593 × CBT + 38.213 × MBT (Sun et al., 2011).

temperatures for the surficial lake bottom sediments range from 23.2–23.8 °C. The average value of 23.1 °C of the local MAT for the past 45 years falls very close this range (Fig. 4). In contrast, the calibration of Pearson et al. (2011) resulted in relatively high temperature estimates for SPM (25.4 °C, 25.0 °C, and 24.9 °C). This phenomenon might be due to the calibration. The calibration of Pearson et al. (2011) was based on lakes from different geographical locations ranging in their latitude from Arctic Scandinavia to Antarctica. Therefore, the calibration model of Sun et al. (2011) was chosen for the reconstruction of paleotemperature in Huguangyan Maar. As shown in Fig. 4, the reconstructed temperatures based on Sun et al. (2011) of the lacustrine material (SPM and bottom sediments) resemble local MAT. Therefore, the calibration of Sun et al. (2011) is considered suitable for paleotemperature reconstruction in Huguangyan Maar.

4.4.2. Temperature estimate for the HGY-2 core 0.3–3.7 ka

The temperature estimates in core HGY-2 range from 24.6 to 26.3 °C based on the global lake-specific calibration of Sun et al. (2011). The down-core variation in the reconstructed temperatures (Fig. 5d) is less than 2 °C, exhibiting a subtle decreasing trend from ~3.7 to 0.3 cal ka BP. These temperatures have the same trends as the results deduced from high-resolution pollen analyses in the same lake (Wang et al., 2007). However, overall the maxima of the temperatures within the Late Holocene show little variation, whereas the minima decreased with time (Fig. 5d).

Comparison of the temperature record of Huguangyan Maar of subtropical South China during the last 0.3–3.7 ka (Section 4.1) with that of Shanghai, Zhejiang and Fujian, East China (Zhang et al., 2000; Liu, 2004) reveals similar trends, although the start time and the duration time of these temperature variations are not synchronous exactly (Fig. 5d and e). The reconstructed temperatures for East China were based on 5 proxy observations of changes in the distribution of temperature-sensitive biota and other climate indices. These include the flowering dates of shrubs, the freezing of rivers, or displacements of the boundary of the farming zones (Zhang, 1996) and documentary data summarized by Chu (1973). As shown in Fig. 5e, the temperature variation in East China during the last three millennia can be divided into nine periods with five cold intervals and four warm intervals (Table 3, Zhang, 1996; Liu, 2004). The air temperature curve of the present study also exhibits nine periods (Fig. 5d), which is consistent with the temperature variation in East China (Zhang, 1996; Liu, 2004) (Fig. 5e). However, the details of temperature variation within the last three millennia using the present reconstructed air temperature in this work differ from that of East China (Liu, 2004, Fig. 5d,e). For instance, during the warm period II, there is a short temperate interval in subtropical southern China while the temperatures remain consistently warm in East China (Zhang, 1996; Liu, 2004). The coldest temperature occurred during period V in East China, but it occurred during period IX in our reconstructed curve (Fig. 5d,e). These discrepancies could be explained by different climatic conditions in East and South China (Wang et al., 2001; Yang et al., 2002).

The warm period VII corresponding to the Medieval Warm Period (MWP, A.D. 900–1300) exhibits warmer temperatures in our record (Fig. 5d). Chu et al. (2002) also deduced a warm phase between 880–1260 AD in the same lake using minerogenic components. However, our reconstructed temperature curve indicates a distinctively different MWP in subtropical South China in which the air temperature is not consistently warmer during the MWP (Fig. 5d). Until now, the opinions on the question "Is there a MWP in China?" are still controversial. For example, Chu (1973) disagreed that a MWP occurred in China according to the Chinese historical documents. However, the records of MWP were found in Central China (Zhang, 1994), North China (Jin et al., 2002), and Taiwan Province (Lou and Chen, 1997). Based on the proxy records from the Chinese historical documents, ice cores, and tree-ring, Wang et al. (2001) suggested that the MWP mainly occurred in East China and that the MWP did not last for more than 400 years. As shown in Fig. 5e, the temperature during the MWP (period VII) displayed a trend from warm to cool and then to warm. *i.e.* the MWP experienced two stages of variations in East China (Zhang, 1996; Zhang et al., 2000; Liu, 2004). However, literature providing MWP records in subtropical/tropical South China is scarce. The paleotemperature estimates of the present study indicate that the MWP occurred in subtropical South China and consisted of two warm periods (Fig. 5d), similar to the record reported from East China.

The coldest period IX in our record might be ascribed to the Little Ice Age. According to the documentary and some tree-ring data, decadal

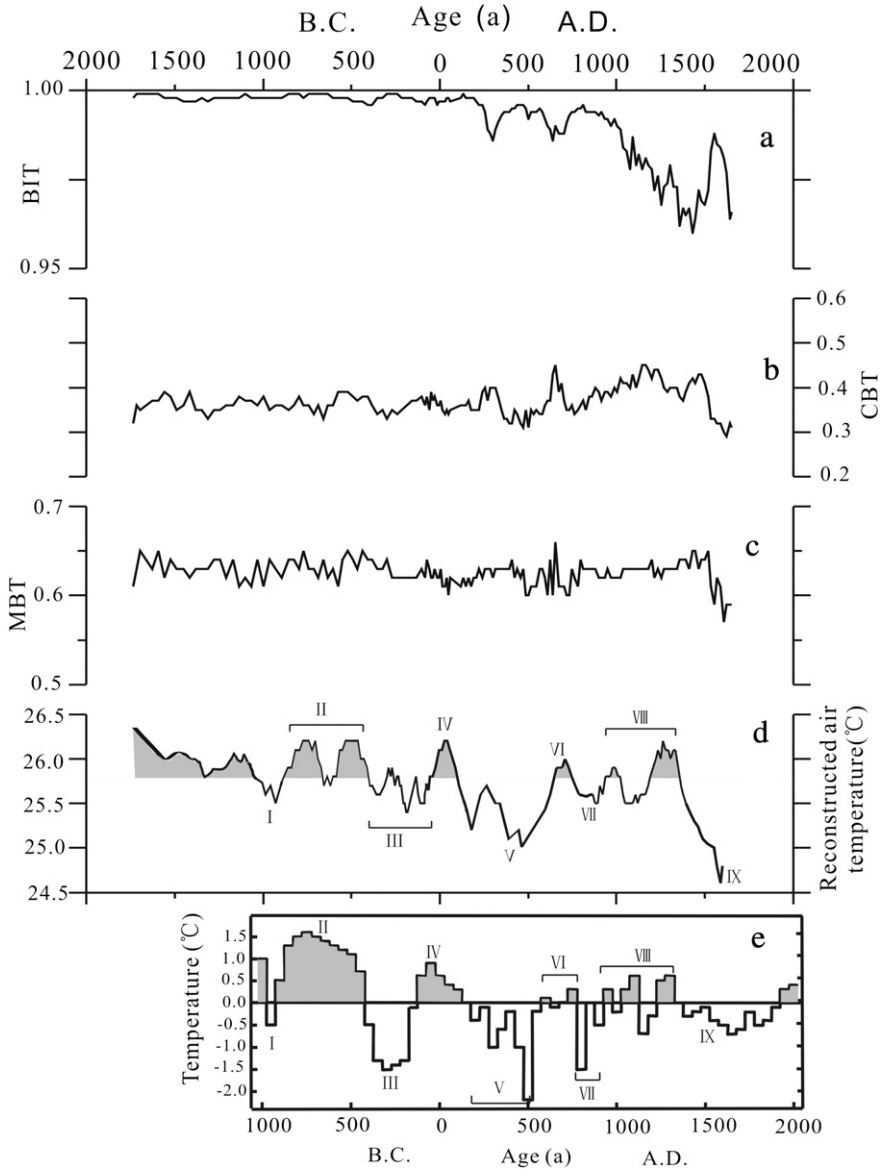

Fig. 5. Profiles of branched GDGT proxies with for core HGY-2: (a) BIT index, (b) CBT values, (c) MBT values, (d) MBT/CBT-reconstructed air temperature, and (e) changes in mean air temperature in East China over the past 3000 years (Liu, 2004 after Zhang et al., 2000).

mean temperature anomaly series were reconstructed for South China (Wang et al., 1998), which suggests the Little Ice Age (1550–1 850 A.D.) occurred in subtropical South China. However, the length and the degree of the cold event vary from region to region in whole China (Wang et al., 1998). Our curve shows that the temperature was the coldest in the Little Ice Age from 0.3–3.7 ka in subtropical South China.

Table 3
The temperature changes in East China over the past 3000 years as compiled from Zhang (1996) and Liu (2004).

Period	Dynasty	Time	Age (ka BP)	Temperature anomaly (°C)	Time of duration (century)
I	Western Zhou	1100–mid 800 BC	3.10–2.80	Cooling (−0.5)	3.5
II	Spring and Autumn	Mid 800–mid 500 BC	2.75–2.45	Warm (+1.0–+1.5)	3.0
III	Warring States–early Western Han	Mid 500–mid 200 BC	2.45–2.15	Cooling (−0.5)	3.0
IV	Mid Western Han–late Eastern Han	Mid 200 BC–late 2nd century AD	2.15–1.80	Warming (+1.0)	3.5
V	Wei, Jin, Northern and Southern	Early 3rd–mid 6th century AD	1.80–1.45	Cold (−0.5)	3.5
VI	Sui–High Tang	Mid 6th–early 8th century AD	1.45–1.25	Temperate (+0.5–+1.0)	2.0
VII	Mid Tang–early Five Dynasties	Mid 8th–late 9th century AD	1.25–1.10	Cold (−0.5)	1.5
VII	Mid Five Dynasties–early Yuan	Early 10th–late 13th century AD	1.10–0.70	Warming (0.5)	4.0
IX	Late Yuan–late Qing	Early 14th–19 th century AD	0.70–0.10	Frigid (−0.5 to −1.0)	6.0

5. Summary, conclusions and their implications

The concentrations and distribution patterns of isoprenoid and branched GDGTs were investigated in the catchment soils, suspended particulate matter (SPM), and bottom sediments of Huguangyan Maar, tropical South China in order to identify the sources of GDGTs, to determine their pathways into the sedimentary archive of the lake, and to test their applicability as paleothermometers on sediment cores from the same lake. The main findings of this study are:

1) Soil and sediments are dominated by branched GDGTs with minor isoprenoid GDGTs. The SPM is dominated by isoprenoid GDGTs with minor branched GDGTs.
2) The distributions of branched GDGTs in SPM and lake surficial sediments are similar but they are different from those of the soil. This relation indicates that the branched GDGTs in Huguangyan Maar sediments are primarily derived from *in situ* production in the lake. Therefore, the reliability of the BIT index suffers from *in situ* production of branched GDGTs in the lake.
3) Of the isoprenoid GDGTs, GDGT-0 is the dominant isoprenoid GDGT in the water column and sediment. However high values of the GDGT-0/crenarchaeol ratio indicate that the isoprenoid GDGTs mainly originate from methanogens in the water column and/or sediment. Therefore, it is not appropriate to use the calculated TEX_{86} values for paleothermometry in the lake.

The above findings lead to the following conclusions:

1) The method based on MBT/CBT to determine paleotemperature was tested and showed that the three SPM samples taken at 0.5, 6 and 18 m water depth gave temperatures of 23.6 °C, 23.2 °C and 22.1 °C, which agreed well with local air temperatures during the sampling periods. The lake bottom sediments yielded temperatures between 23.2 and 23.8 °C, which are close to the MAT value of the measured local temperature (23.1 °C) for the preceding 45 years. This agreement indicates the feasibility of using MBT/CBT for paleothermometry in Huguangyan Marr and similar lacustrine settings.
2) The distribution of the branched DGGTs and the temperatures calculated from the MBT/CBT ratios using the global lake specific calibrations for the provided a temperature record of 0.3–3.7 ka span.
3) This temperature record of the cores of the Huguangyang Maar consists of distinct periods: four warm and five cold. Moreover, It clearly resolved details of the Medieval Warm Period (900–1300 AD) in identifying two distinct warm intervals for this period. Furthermore, the coldest temperature recorded prevailed during the Little Ice Age, in subtropical South China. This paleotemperature profile is similar to that of East China as derived from other indicators.

This study has wider implications for paleoclimate investigations of lake sediments. Although the exact biological origin of branched DGGTs is not yet known, the present study of the SPM, lake bottom sediments and a 0.3–3.7 ka core in the Huguangyan Maar shows that they originate within the water body and not from the soil. Hence they can be used as reliable temperature indicators in sediments deposited in similar lacustrine settings that have a dominance of branched DGGTs produced *in situ*.

Supplementary data to this article can be found online at http://dx.doi.org/10.1016/j.palaeo.2015.06.014.

Acknowledgments

We would like to thank Dr. Luhua Xie and Mr Ti Zeng for help with fieldwork and Jiazhuo He for analytical assistance with the HPLC-MS equipment. We would like to thank Editage for providing editorial assistance. Professor Phil Meyers provided useful comments on an earlier version of this manuscript. This work was financially supported by a GIGCAS 135 project Y234091001 and Natural Science Foundation of China (Nos. 41072264 and 40930106) and this is also Contribution No.IS-2090 from GIGCAS.

References

Blaga, C.I., Reichart, G.J., Heiri, O., Sinninghe Damsté, J.S., 2009. Tetraether membrane lipid distributions in water-column particulate matter and sediments: a study of 47 European lakes along a north–south transect. J. Paleolimnol. 41, 523–540.
Blaga, C.I., Reichart, G.J., Schouten, S., Lotter, J.P., Werne, A.F., Kosten, S., Mazzeo, N., Lacerot, G., Sinninghe Damsté, J.S., 2010. Branched glycerol dialkyl glycerol tetraethers in lake sediments: can they be used as temperature and pH proxies? Org. Geochem. 41, 1225–1234.
Castañeda, I.S., Schouten, S., 2011. A review of molecular organic proxies for examining modern and ancient lacustrine environments. Quat. Sci. Rev. 30, 2851–2891.
Chu, K.C., 1973. A preliminary study on the climatic fluctuations during the last 5000 years in China. Sci. Sin. XVI 2, 226–256.
Chu, G.Q., Liu, J.Q., Sun, Q., Lü, H.Y., Gu, Z.Y., Wang, W.Y., Liu, T.S., 2002. The 'Mediaeval Warm Period' drought recorded in Lake Huguangyuan, tropical South China. The Holocene 12, 511–516.
De Rosa, M., Gambacorta, A., 1988. The lipids of archaebacteria. Prog. Lipid Res. 27, 153–175.
Fawcett, P.J., Werne, J.P., Anderson, R.S., Heikoop, J.M., Brown, E.T., Berke, M.A., Smith, S.J., Goff, F., Donohoo-Hurley, L., Cisneros-Dozal, L.M., Schouten, S., Sinninghe Damsté, J.S., Huang, Y.S., Toney, J., Fessenden, J., WoldeGabriel, G., Atudorei, V., Geissman, J.W., Allen, C.D., 2011. Extended megadroughts in the southwestern United States during Pleistocene interglacials. Nature 470, 518–521.
Ge, Q.S., Zheng, J.Y., Fang, X.Q., Man, Z.M., Zhang, X.Q., Zhang, P.Y., Wang, W.C., 2003. Winter half-year temperature reconstruction for the middle and lower reaches of the Yellow River and Yangtze River, China, during the past 2000 years. The Holocene 13 (6), 933–940.
Guo, Z., Wang, J., Chai, M., Chen, Z., Zhan, Z., Zheng, W., Wei, X., 2011. Spatiotemporal variation of soil pH in Guangdong Province of China in past 30 years. Chin. J. Appl. Ecol. 22 (2), 425–430.
Hopmans, E.C., Weijers, J.W.H., Schefuss, E., Herfort, L., Sinninghe Damsté, J.S., Schouten, S., 2004. A novel proxy for terrestrial organic matter in sediments based on branched and isoprenoid tetraether lipids. Earth Planet. Sci. Lett. 224, 107–116.
Huguet, C., Hopmans, E.C., Febo-Ayala, W., Thompson, D.H., Sinninghe Damsté, J.S., Schouten, S., 2006. An improved method to determine the absolute abundance of glycerol dibiphytanyl glycerol tetraether lipids. Org. Geochem. 37, 1036–1041.
Jin, Z.D., Shen, J., Wang, S.M., Zhang, E.L., 2002. The medieval warm period in the Daihai Area. J. Lake Sci. 14, 209–216 (in Chinese with English abstract).
Koga, Y., Morii, H., 2006. Special methods for the analysis of ether lipid structure and metabolism in archaea. Anal. Biogeochemistry 348, 1–14.
Liu, J.Q., 1999. Volcanoes in China. Science Press of China, Beijing.
Liu, T.S., 2004. Climate Process and Change. Science Press of China, Beijing, pp. 236–238.
Loomis, S.E., Russell, J.M., Sinninghe Damsté, J.S., 2011. Distributions of branched GDGTs in soils and lake sediments from western Uganda: implications for a lacustrine paleothermometer. Org. Geochem. 42, 739–751.
Loomis, S.E., Russell, J.M., Ladd, B., Street-Perrott, F.A., Sinninghe Damsté, J.S., 2012. Calibration and application of the branched GDGT temperature proxy on East African lake sediments. Earth Planet. Sci. Lett. 357–358, 277–288.
Lou, J.Y., Chen, C.T.A., 1997. Paleoclimatological and paleoenvironmental records since 4000 BP in the sediments of alpine lakes in Taiwan. Sci. China (D) 40 (4), 424–431.
Lund, S.P., Stott, L., Schwartz, M., Thunell, R., Chen, A., 2006. Holocene paleomagnetic secular variation records from the western Equatorial Pacific Ocean. Earth Planet. Sci. Lett. 246, 381–392.
Mingram, J., Schettlera, G., Nowaczyk, N., Luo, X., Lü, H., Liu, J., Negendank, J.F.W., 2004. The Huguang maar lake—a high-resolution record of palaeoenvironmental and palaeoclimatic changes over the last 78,000 years from South China. Quat. Int. 122, 85–107.
Naeher, S., Peterse, F., Smittenberg, R.H., Niemann, H., Zigah, P.K., Schubert, C.J., 2014. Sources of glycerol dialkyl glycerol tetraethers (GDGTs) in catchment soils, water column and sediments of Lake Rotsee (Switzerland)—implications for the application of GDGT-based proxies for lakes. Org. Geochem. 66, 164–173.
Ochsenreiter, T., Selezi, D., Quaiser, A., Bonch-Osmolovskaya, L., Schleper, C., 2003. Diversity and abundance of Crenarchaeota in terrestrial habitats studied by 16S RNA surveys and real time PCR. Environ. Microbiol. 5, 787–797.
Pearson, E.J., Juggins, S., Talbot, H.M., Weckström, J., Rosén, P., Ryves, D.B., Roberts, S.J., Schmidt, R., 2011. A lacustrine GDGT-temperature calibration from the Scandinavian Arctic to Antarctic: renewed potential for the application of GDGT-paleothermometry in lakes. Geochim. Cosmochim. Acta 75, 6225–6238.
Pitcher, A., Rychlik, N., Hopmans, E.C., Spieck, E., Rijpstra, W.I.C., Ossebaar, J., Schouten, S., Wagner, M., Sinninghe Damsté, J.S., 2010. Crenarchaeol dominates the membrane lipids of *Candidatus Nitrososphaera gargensis*, a thermophilic Group I 1b Archaeon. ISME J. 4, 542–552.
Pitcher, A., Hopmans, E.C., Mosier, A.C., Park, S.J., Rhee, S.K., Francis, C.A., Schouten, S., Sinninghe Damsté, J.S., 2011. Core and intact polar glycerol dibiphytanyl glycerol tetraether lipids of ammonia-oxidizing Archaea enriched from marine and estuarine sediments. Appl. Environ. Microbiol. 77, 3468–3477.
Powers, L.A., Werne, J.P., Johnson, T.C., Hopmans, E.C., Sinninghe Damsté, J.S., Schouten, S., 2004. Crenarchaeotal membrane lipids in lake sediments: a new paleotemperature proxy for continental paleoclimate reconstruction? Geology 32, 613–616.

Powers, L.A., Johnson, T.C., Werne, J.P., Castañeda, I.S., 2005. Large temperature variability in the southern African tropics since the Last Glacial Maximum. Geophys. Res. Lett. 32 (L08706-1-4).

Powers, L.A., Werne, J.P., Vanderwoude, A.J., Sinninghe Damsté, J.S., Hopmans, E.C., Schouten, S., 2010. Applicability and calibration of the TEX_{86} paleothermometer in lakes. Org. Geochem. 41, 404–413.

Schouten, S., Hopmans, E.C., Schefub, E., Sinninghe Damsté, J.S., 2002. Distributional variations in marine crenarchaeotal membrane lipids: a new organic proxy for reconstructing ancient sea water temperatures? Earth Planet. Sci. Lett. 204, 265–274.

Schouten, S., Huguet, C., Hopmans, E.C., Kienhuis, M.V.M., Sinninghe Damsté, J.S., 2007. Analytical methodology for TEX_{86} paleothermometry by high-performance liquid chromatography/atmospheric pressure chemical ionization-mass spectrometry. Anal. Chem. 79, 2940–2944.

Schouten, S., Hopmans, E.C., Baas, M., Boumann, H., Standfest, S., Könneke, M., Stahl, D.A., Sinninghe Damsté, J.S., 2008. Intact membrane lipids of "*Candidatus Nitrosopumilus maritimus*", a cultivated representative of the cosmopolitan mesophilic group I crenarchaeota. Appl. Environ. Microbiol. 74, 2433–2440.

Schouten, S., Hopmans, E.C., Sinninghe Damsté, J.S., 2013. The organic geochemistry of glycerol dialkyl glycerol tetraether lipids: a review. Org. Geochem. 54, 19–61.

Sinninghe Damsté, J.S., Hopmans, E.C., Pancost, R.D., Schouten, S., Geenevasen, J.A.J., 2000. Newly discovered non-isoprenoid glycerol dialkyl glycerol tetraether lipids in sediments. Chem. Commun. 1683–1684.

Sinninghe Damsté, J.S., Hopmans, E.C., Schouten, S., van Duin, A.C.T., Geenevasen, J.A.J., 2002. Crenarchaeol: the characteristic core glycerol dibiphytanyl glycerol tetraether membrane lipid of cosmopolitan pelagic crenarchaeota. J. Lipid Res. 43, 1641–1651.

Sinninghe Damsté, J.S., Rijpstra, W.I.C., Hopmans, E.C., Weijers, J.W.H., Foesel, B.U., Overmann, J., Dedysh, S.N., 2011. 13,16-Dimethyl octacosanedioic acid (isodiabolic acid), a common membrane-spanning lipid of Acidobacteria subdivisions 1 and 3. Appl. Environ. Microbiol. 77, 4147–4154.

Sinninghe Damsté, J.S., Rijpstra, W.I.C., Hopmans, E.C., Man-Young, Jung, Jong-Geol, Kim, Rhee, S.-K., Stieglmeier, M., Schleper, C., 2012. Intact polar and core glycerol dibiphytanyl glycerol tetraether lipids of group 1.1a and 1.1b ammonia-oxidizing archaea in soil. Appl. Environ. Microbiol. 78, 6866–6874.

Sun, Q., Chu, G., Liu, M., Xie, M., Li, S., Ling, Y., Wang, X., Shi, L., Jia, G., Lǘ, H., 2011. Distribution and temperature dependence of branched glycerol dialkyl glycerol tetraethers in recent lacustrine sediments from China and Nepal. J. Geophys. Res. 116, G01008. http://dx.doi.org/10.1029/2010JG001365.

Tierney, J.E., Russell, J.M., 2009. Distributions of branched GDGT in a tropical lake system: implications for lacustrine application of the MBT/CBT paleoproxy. Org. Geochem. 40, 1032–1036.

Tierney, J.E., Russell, J.M., Huang, Y.S., Sinninghe Damsté, J.P., Hopmans, E.C., Cohen, A.S., 2008. Northern hemisphere controls on tropical Southeast African climate during the past 60,000 years. Science 322, 252–255.

Tierney, J.E., Russell, J.M., Eggermont, H., Hopmans, E.C., Verschuren, D., Sinninghe Damsté, J.S., 2010. Environmental controls on branched tetraether lipid distributions in tropical East African lake sediments. Geochim. Cosmochim. Acta 74, 4902–4918.

Walsh, E.M., Ingalls, A.E., Keil, R.G., 2008. Sources and transport of terrestrial organic matter in Vancouver Island fjords and the Vancouver–Washington Margin: a multiproxy approach using δ^{13}Corg, lignin phenols, and the ether lipid BIT index. Limnol. Oceanogr. 53, 1054–1063.

Wang, S.W., Ye, J.L., Gong, D.Y., 1998. Climate in China during the Little Ice Age. Quat. Sci. 1, 54–62 (in Chinese with English abstract).

Wang, W.Y., Liu, J.Q., Liu, T.S., Peng, P.A., Lu, H.Y., Gu, Z.Y., Chu, G.Q., Negendank, J., Luo, X.J., Mingram, J., 2000. The two-step monsoon changes of the last deglaciation recorded in tropical Maar Lake Huguangyan, southern China. Chin. Sci. Bull. 45, 1529–1532.

Wang, S.W., Gong, D.Y., Zhu, J.H., 2001. Twentieth-century climatic warming in China in the context of the Holocene. The Holocene 11, 313–321.

Wang, S.Y., Lü, H.Y., Liu, J.Q., Negendank, J.F.W., 2007. The early Holocene optimum inferred from a high-resolution pollen record of Hugaungyan Maar Lake in southern China. Chin. Sci. Bull. 52 (20), 2829–2836.

Wang, L., Li, J.J., Lü, H.Y., Gu, Z.Y., Rioual, P., Hao, Q.Z., Mackay, A.W., Jiang, W.Y., Cai, B.G., Xu, B., Han, J.T., Chu, G.Q., 2012. The East Asian winter monsoon over the last 15,000 years: its links to high-latitudes and tropical climate systems and complex correlation to the summer monsoon. Quat. Sci. Rev. 32, 131–142.

Weijers, J.W.H., Schouten, S., Hopmans, E.C., Geenevasen, J.A.J., David, O.R.P., Coleman, J.M., Pancost, R.D., Sinninghe Damsté, J.S., 2006a. Membrane lipids of mesophilic anaerobic bacteria thriving in peats have typical archaeal traits. Environ. Microbiol. 8, 648–657.

Weijers, J.W.H., Schouten, S., Spaargaren, O.C., Sinninghe Damsté, J.S., 2006b. Occurrence and distribution of tetraether membrane lipids in soils: implications for the use of the TEX_{86} proxy and the BIT index. Org. Geochem. 37, 1680–1693.

Weijers, J.W.H., Schefuβ, E., Schouten, S., Sinninghe Damsté, J.S., 2007a. Coupled thermal and hydrological evolution of tropical Africa over the last deglaciation. Science 315, 1701–1703.

Weijers, J.W.H., Schouten, S., van den Donker, J.C., Hopmans, E.C., Sinninghe Damsté, J.S., 2007b. Environmental controls on bacterial tetraether membrane lipid distribution in soils. Geochim. Cosmochim. Acta 71, 703–713.

Yancheva, G., Nowaczyk, N.R., Mingram, J., Dulski, P., Schettler, G., Negendank, J.F.W., Liu, J., Sigman, D.M., Peterson, L.C., Haug, G.H., 2007. Influence of the intertropical convergence zone on the East Asian monsoon. Nature 445, 74–77.

Yang, B., Braeuning, A., Johnson, K.R., Shi, Y.F., 2002. General characteristics of temperature variation in China during the last two millennia. Geophys. Res. Lett. 29 (38-31–38-34).

Yang, X.Q., Heller, F., Yang, J., Su, S.H., 2009. Paleosecular variations since ~ 9000 yr BP as recorded by sediments from maar lake Shuangchiling, Hainan, South China. Earth Planet. Sci. Lett. 288, 1–9.

Yang, X.Q., Liu, Q.S., Duan, Z.Q., Su, Z.H., Wei, G.J., Jia, G.D., Ouyang, T.P., Su, Y.L., Xie, L.H., 2012. A Holocene palaeomagnetic secular variation record from Huguangyan maar Lake, southern China. Geophys. J. Int. 190, 188–200.

Zhang, D., 1994. Evidence for the existence of the Medieval Warm Period in China. Clim. Chang. 26, 289–297.

Zhang, P.Y., 1996. Chinese Historical Climate Change. In: Yafeng, Shi (Ed.), Shandong Science and Technology Press, Ji'nan, p. 533.

Zhang, L.S., Fang, X.Q., Ren, G.Y., 2000. Global Change. Higher Education Press, Beijing, p. 431.

Zheng, Z., Lei, Z., 1999. A 400,000 year record of vegetational and climatic changes from a volcanic basin, Leizhou Peninsula, southern China. Palaeogeogr. Palaeoclimatol. Palaeoecol. 145, 339–362.

Zhou, H.D., Hu, J.F., Spiro, B., Peng, P.A., Tang, J.H., 2014. Glycerol dialkyl glycerol tetraethers in surficial coastal and open marine sediments around China: indicators of sea surface temperature and effects of their sources. Palaeogeogr. Palaeoclimatol. Palaeoecol. 395, 114–121.

Zink, K.G., Vandergoes, M.J., Mangelsdorf, K., Dieffenbacher-Krall, A.C., Schwark, L., 2010. Application of bacterial glycerol dialkyl glycerol tetraethers (GDGTs) to develop modern and past temperature estimates from New Zealand lakes. Org. Geochem. 41, 1060–1066.